Nanoscale

PAPER

View Article Online
View Journal | View Issue



Cite this: *Nanoscale*, 2017, **9**, 14907

# Localized plasmonic structured illumination microscopy with an optically trapped microlens†

Anna Bezryadina,[a] Jinxing Li,[b] Junxiang Zhao,[a] Alefia Kothambawala,[a] Joseph Ponsetto,[a] Eric Huang,[c] Joseph Wang[b] and Zhaowei Liu*[a]

Received 23rd May 2017,
Accepted 3rd September 2017

DOI: 10.1039/c7nr03654j

rsc.li/nanoscale

Localized plasmonic structured illumination microscopy (LPSIM) is a recently developed super resolution technique that demonstrates immense potential *via* arrays of localized plasmonic antennas. Microlens microscopy represents another distinct approach for improving resolution by introducing a spherical lens with a large refractive index to boost the effective numerical aperture of the imaging system. In this paper, we bridge together the LPSIM and optically trapped spherical microlenses, for the first time, to demonstrate a new super resolution technique for surface imaging. By trapping and moving polystyrene and $TiO_2$ microspheres with optical tweezers on top of a LPSIM substrate, the new imaging system has achieved a higher NA and improved resolution.

## Introduction

The development of the optical microscope revolutionized life and materials science; however, the resolution of conventional microscopes is limited to the half-wavelength scale (200–300 nm) due to the diffractive nature of the illuminating light. In modern medicine and biology there is a strong demand for surface imaging of various objects and processes at size scales far below the diffraction limit of visible light. Recent super resolution microscopy techniques, such as stimulated emission depletion microscopy (STED),[1–3] stochastic optical reconstruction microscopy (STORM),[4,5] and photo-activated localization microscopy (PALM)[6] have been demonstrated and attracted much attention. These methods have greatly improved the spatial resolution to sub-50 nm scales in all three dimensions, but at the cost of other imaging capabilities such as imaging speed, field of view and simplicity of the system, as well as phototoxicity. Structured illumination microscopy (SIM)[7–11] can achieve a reasonable speed and wide field of view simultaneously, but its resolution is limited to ~2 times better than the diffraction limit, *i.e.* about 84 nm when in combination with total internal reflection fluorescence (TIRF) and the best available ultrahigh NA objective.[12]

Recently, plasmonics has been introduced to the field of SIM to further improve its resolution. For instance, plasmonic structure illumination microscopy (PSIM) utilizes the surface plasmon interference to replace the traditional projected light pattern, so that the resolution improvement can surpass 2 times that of the diffraction limit.[13–16] Localized plasmon structured illumination microscopy (LPSIM) employs near-field excitation from the localized surface plasmons of fine periodic structures.[17,18] With this unique super resolution technique and 1.2NA objective, wide-field surface imaging with resolution down to 75 nm was demonstrated. This represents ~3 times resolution improvement compared with conventional epi-fluorescence microscopy, while maintaining reasonable speed and compatibility with biological specimens.[18] Both PSIM and LPSIM also rely on the spatial frequency mixing between the illumination patterns and the object, therefore the super resolution image must be numerically reconstructed using a SIM[19] or blind SIM reconstruction method.[14,18,20] The resonant plasmonic enhancement of the localized plasmonic fields provides strong excitation of targeted fluorescent labels, which allows shorter exposure times and thus faster imaging speeds.

Currently, all SIM technologies are using commercial objectives for image collection, so that the objective NA becomes a major limiting factor. Combining dielectric microspheres with low NA objectives has been proven as a valuable scheme to improve the effective NA of the imaging system for resolving much finer structures.[21–28] By placing high-index dielectric microspheres close to the investigation surface, near-field coupling occurs and an extraordinary sharp focus (so-called

[a]*Department of Electrical and Computer Engineering, University of California, San Diego, La Jolla, California 92093, USA. E-mail: zhaowei@ucsd.edu*
[b]*Department of Nanoengineering, University of California, San Diego, La Jolla, California 92093, USA*
[c]*Department of Physics, University of California, San Diego, La Jolla, California 92093, USA*

† Electronic supplementary information (ESI) available: Video files showing trapping and moving 46 μm polystyrene spheres and 17 μm $TiO_2$ spheres with optical tweezers. See DOI: 10.1039/c7nr03654j

"photonic nanojet") with local strongly enhanced imaging has been demonstrated.[23,24,27] Although the mechanisms for this enhanced resolution have been debated in the literature,[22–25,28] it is commonly believed that the high refractive index of the microlenses increases the total effective NA of the imaging system, leading to the improved resolution. For practical applications, the microlenses typically need to be mobile to reach the desired location, which can be guided by fine glass micropipettes,[29] optical tweezers,[30–37] electrostatic attachment to an AFM tip[38] or chemical propulsion.[39] In this paper, by combining a near-field microlens with LPSIM for the first time, we report a new microscopy technique which offers advantages over existing super-resolution imaging methods with significantly improved resolution.

## Experimental

### Experimental set-up

The schematic diagram of the new microscopy system, *i.e.* optical tweezers based LPSIM (OT-LPSIM), is shown in Fig. 1. For the LPSIM illumination part of the system, the excitation laser beam passes through two galvanometer scanning mirrors, a lens and a microscope objective in a 4f system, and then illuminates the plasmonic substrate, creating the plasmonic structured illumination excitation pattern. The beam polarization and illumination angle incident to the plasmonic structure were controlled by radially orientated polarizer strips (in front of the objective) and the galvo scanners, respectively. The fluorescence emission excited by the plasmonic structure was collected by the microsphere and an objective, and forms diffraction-limited images at the CCD camera (see Fig. 2a). The trapped microsphere acts like a movable microlens and allows the user to interactively zoom into the field of interest together with the objective. For the optical trapping and manipulation of the microsphere we use a continuous wave 825 nm laser (20–30 mW), which is compatible for future biological applications and has low optical damage.[31,40] The collimated expanded infrared (IR) laser was emitted from the top and focused on the observation plane by the same imaging objective.

The LPSIM substrates we used include a hexagon lattice array of 60 nm silver discs with a 150 nm pitch embedded in silica, as shown in Fig. 2b. When polarized laser light hits the

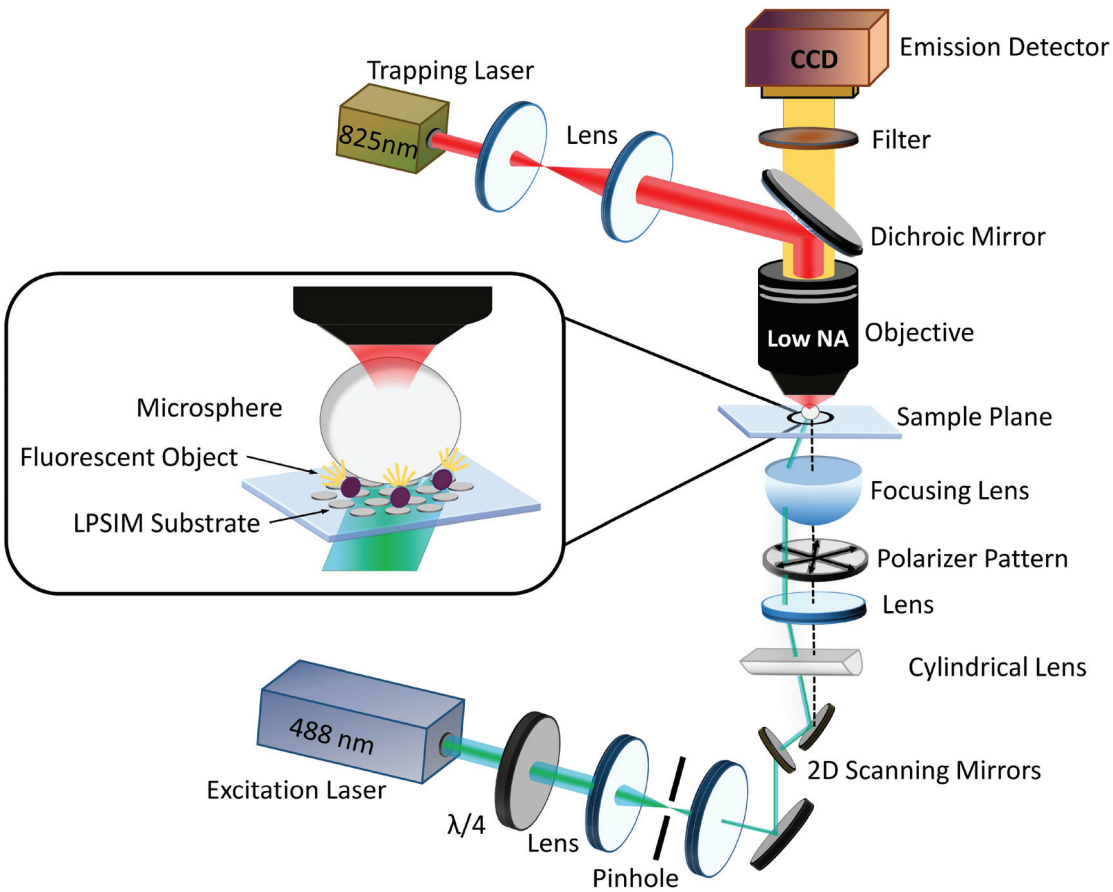


**Fig. 1** Schematic diagram of the OT-LPSIM experimental setup. An excitation laser is directed *via* 2D scanning mirrors through a 4f system which defines the angle of laser incidence to the LPSIM substrate. In-plane polarization regardless of angle is guaranteed by a custom-made polarizer plate, which ensures the correct excitation patterns. An IR trapping laser is used to move and control the position of the microlens. The emitted fluorescence is collected through the microlens, then the objective, filtered, and passed to the emission detector CCD.

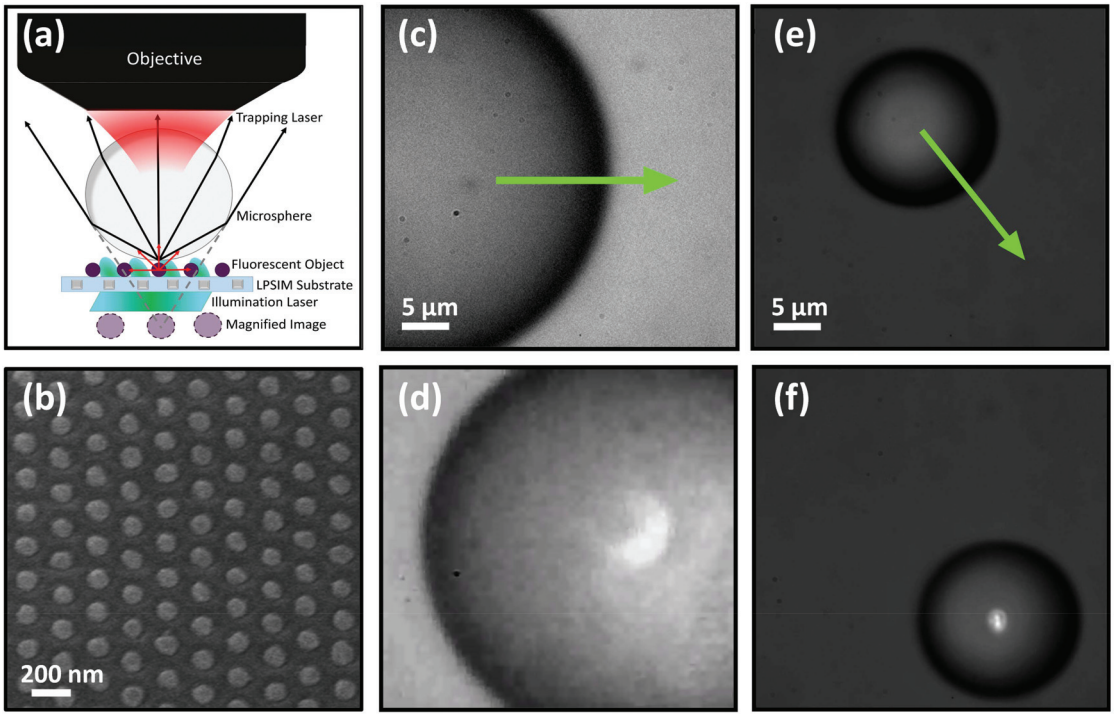


Fig. 2 (a) Schematic of the microsphere-assisted imaging setup integrated with LPSIM. (b) SEM image of the nanodisc array in the LPSIM substrate, showing 60 nm silver discs arranged in a hexagonal lattice. (c, d) Image of 46 μm polystyrene microsphere being trapped by the optical tweezers' IR beam (see ESI Media 1†). (e, f) Image of 17 μm $TiO_2$ microsphere being trapped by optical tweezers' IR beam (see ESI Media 2†).

plasmonic nano-disc array, it creates evanescent fields which illuminate fluorescent objects in the near field.[18] By optically trapping the microsphere lens on top of the LPSIM substrate with fluorescent objects, the LPSIM sub-images are further magnified and collected by a much higher effective NA of the system, leading to greatly improved LPSIM resolution while using a relatively low NA objective.

### Optically controlled microspheres

By altering the sizes and materials of microspheres immersed in varied liquids, we could achieve different effective NAs, resolutions, and magnifications below a sphere.[25] The image magnification of the sphere, can be roughly approximated by geometric optics $M = n_r/(2 - n_r)$, where $n_r$ is a relative index contrast of the microsphere and the surrounding medium.[22] For the best imaging quality, the optimal relative index contrast $n_r$ between the microsphere and medium is 1.4–1.75.[22,23] The polystyrene spheres (the index of refraction $n$ = 1.59) in water ($n$ = 1.33) have low relative index contrast 1.2, but they are commercially available in a vast range of sizes and can be easily optically trapped.[34,36] The $TiO_2$ spheres ($n$ = 2.1) in water have optimal relative index contrast 1.58 for imaging, but according to the theoretical predictions the particle trapping efficiency could strongly depend on the sphere size.[34] The theoretical magnifications for polystyrene and $TiO_2$ spheres are 1.48 and 3.76, respectively. Since the spheres are micro-sized, for the same material the real experimental magnification non-linearly varies with the sphere's radius.[24,25] Also to move a microsphere with optical tweezers without disturbing the sample, we need to have a tiny gap between the microsphere and the LPSIM substrate, which could also slightly affect the magnification.[41] So for different sphere sizes, the magnification properties can vary and should be estimated experimentally.

For our experiment, we primarily used two types of microspheres: ~45 μm diameter polystyrene spheres with 1.55 magnification and ~20 μm $TiO_2$ spheres with 3.6 magnification, both of which are optically trapped in water and free to be moved to the desired area. The exact magnification for each sphere was estimated by measuring the distances between fluorescent beads with and without a sphere in front of them. In Fig. 2c–f and ESI Media 1 and Media 2† we demonstrated the trapping and movement of both types of spheres with optical tweezers. Larger spheres were later used to maximize the magnified area below the sphere and to demonstrate the performance of OT-LPSIM. In general, 30% of the area below the center of the sphere can be safely used for reconstruction without much aberration.

## Results and discussion

### Polystyrene microspheres

To test the super-resolution imaging performance of our OT-LPSIM system, 40 nm fluorescent beads (570 nm emission) were drop-casted and fixed onto the LPSIM substrate, and were

imaged through a 46 μm polystyrene microsphere. The polystyrene sphere can be trapped and moved into the area of interest (Fig. 3a–c) at significantly lower laser power, since the sphere was not only trapped by the direct laser beam from the objective but also by the reflected beam from the metallic nano-array. The fluorescence was excited by a 488 nm laser and imaged with a 0.8NA 60× air objective.

The resolving capacity of OT-LPSIM was demonstrated by the FWHM of a single-bead at the same location for a diffraction-limited image without a sphere, under a sphere, and after LPSIM reconstruction without a sphere and under a sphere (see Fig. 3d, e, g and h), respectively. Theoretically, an objective with NA = 0.8 should have resolution around 435 nm but this objective was used far from its optimized condition in this specific experiment, leading to a lesser resolution to 625 nm. Nevertheless, the effective NA of the system with the microlens was improved to 1.0 according to the Rayleigh criterion $NA_{eff} = 0.61\lambda/FWHM$, where $\lambda$ is the emission wavelength and FWHM can be found from the experimental data. The polystyrene sphere improved the diffraction limited images of the fluorescence beads by 1.8 times, allowing greater visibility of fine details, and decreased the FWHM from 625 nm down to 350 nm. After applying the LPSIM reconstruction method for a regular diffraction-limited image without the microlens, the FWHM decreased more than 3 times, down to 195 nm. For the image under the microlens after LPSIM reconstruction, the final FWHM dropped to 90 nm, representing 7-times resolution enhancement compared to the diffraction limited image obtained from the objective only (Fig. 3f). In Fig. 3i, it is clearly seen that two closely-spaced beads, which appeared as one bright spot in Fig. 3d, e, and g, were resolved with the OT-LPSIM technique. The center to center distance of the beads was 130 nm, which means that the edge-to-edge gap between two beads was 90 nm.

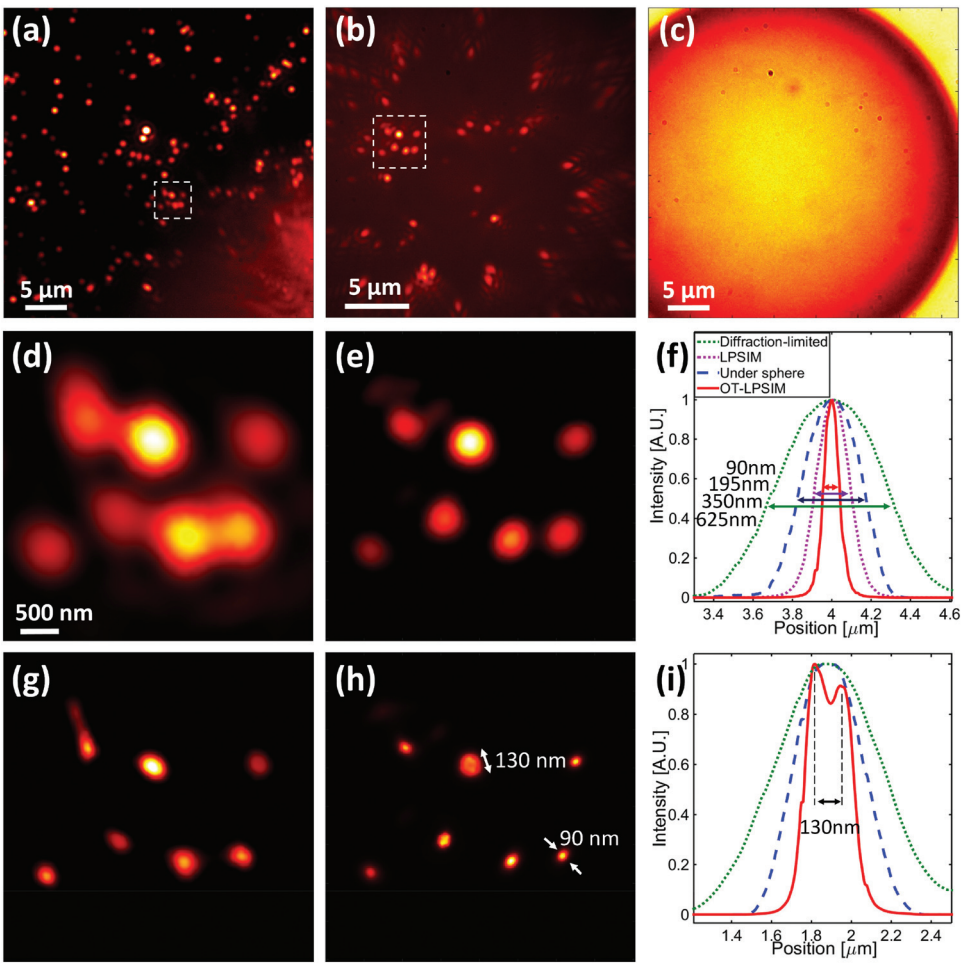


**Fig. 3** (a) Fluorescence image of 40 nm beads through a 60× (0.8NA) objective lens at 488 nm excitation. (b) Fluorescent beads are magnified 1.55 times under a polystyrene microsphere. The microscope objective was focused on the virtual images formed underneath the sphere. (c) Image of 46 μm diameter movable polystyrene sphere. (d) Diffraction-limited image of the selected area in (a). (e) Corresponding magnified image of (b) under microlens with significantly improved resolution. (g) LPSIM reconstructed image of (d). (h) OT-LPSIM reconstructed image of (e). (f, i) Quantification of the experimental resolution in (d, e, g, h) using the intensity profile. Standard FWHM: 625 nm; FWHM with microlens: 350 nm; LPSIM FWHM: 195 nm; OT-LPSIM FWHM: 90 nm.

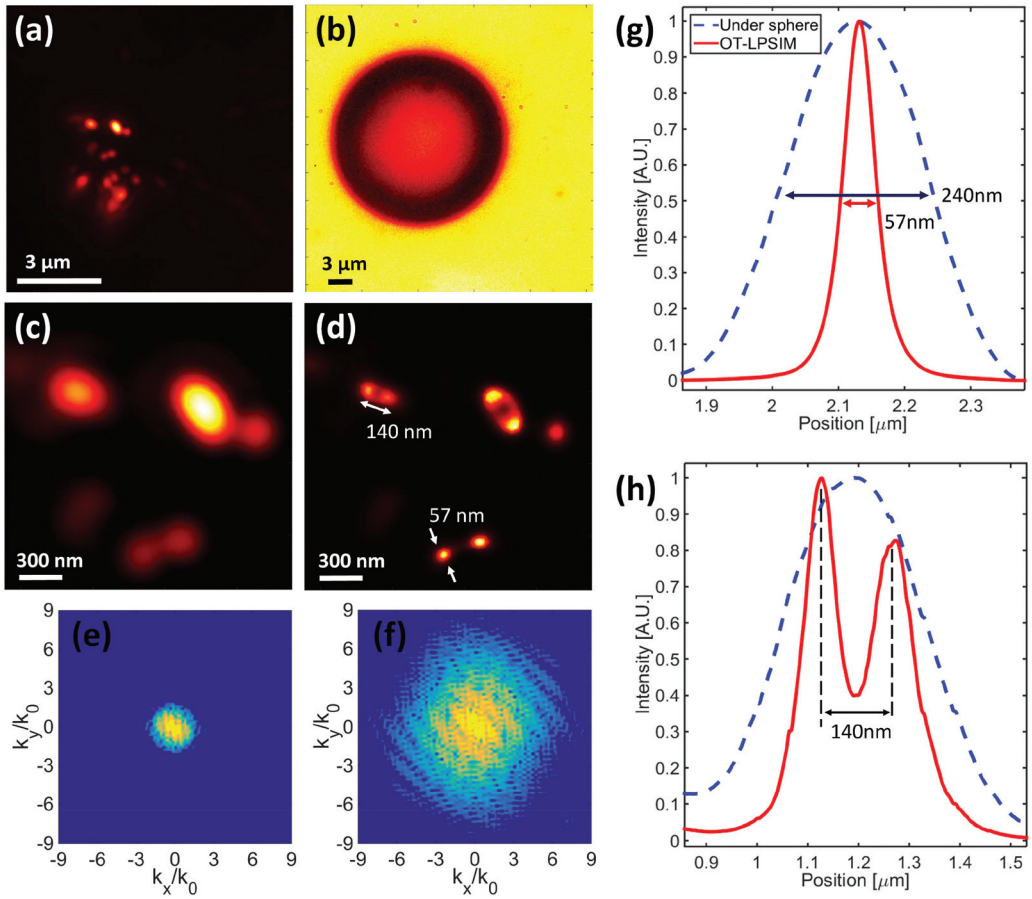


**Fig. 4** (a) Magnified fluorescence image of 40 nm diameter beads under $TiO_2$ microsphere through 60× (0.8NA) objective lens. (b) Image of a 21 μm movable $TiO_2$ microsphere. (c) Selected area of a fluorescent bead under a sphere. The image is magnified 3.6 times under a $TiO_2$ sphere. (d) OT-LPSIM reconstructed image of a selected area. (e, f) Spatial frequency spectra (log-scale amplitude) of images under sphere before and after LPSIM reconstruction, respectively. The $k_0$ is the free space wavevector. (g, h) Quantification of the experimental resolution using the intensity profile. The FWHM after LPSIM reconstruction drops to 57 nm.

### $TiO_2$ microspheres

With optically trapped $TiO_2$ microspheres on top of the LPSIM substrate, we achieved even bigger improvement of resolution. For the experiment, the same 40 nm fluorescent beads were fixed onto a LPSIM substrate with 21 μm $TiO_2$ microspheres in water on top of it. As the $TiO_2$ sphere was moved with the IR optical trapping laser, the area below the microsphere was magnified 3.6 times, as shown in Fig. 4a and b. The effective NA of the system increased to 1.45NA and the diffraction-limited FWHM under the sphere decreased from 625 nm to 240 nm.

Significantly, after applying the LPSIM technique, multiple clusters of beads under the $TiO_2$ microsphere were resolved even farther, allowing distinct separation between neighboring beads, as shown in Fig. 4c and d. After LPSIM reconstruction, the FWHM decreased, from 240 nm under the microlens, to 57 nm ($\sim\lambda/10$), which provided an additional 4.2 times improvement of the $TiO_2$ microlens (Fig. 4g). As a result, if we compare our experimental diffraction-limited FWHM without a sphere produced by an objective slightly away from its optimal position (Fig. 3a and f) and the final FWHM with OT-LPSIM using $TiO_2$ microspheres (Fig. 4d and g), the corresponding resolution improvement is ~11 times. Fig. 4e and f show the corresponding Fourier space spectrum under the microsphere with and without the LPSIM technique applied, which confirms the expected resolution improvement before and after LPSIM reconstruction.

## Conclusions

In this work we demonstrated how the combination of an optically trapped microlens with LPSIM can boost the effective numerical aperture of the imaging system and improve the resolution of the existing super-resolution technique. We selected two types of microlens with different sizes and materials: polystyrene microspheres with a relatively smaller index of refraction and $TiO_2$ microspheres with a higher index, both can be optically trapped and manipulated to the desired location. With this new microscopy technique, we achieved 7–11 times improvement of FWHM compared with experi-

mental diffraction-limited FWHM using solely the objective. We believe that the resolution could be easily improved even further by using a long working distance objective, alternative microspheres, shorter operational wavelengths, and more optimal LPSIM substrates. The OT-LPSIM provides a new super resolution approach that may have great potential for various imaging applications.

## Conflicts of interest

There are no conflicts to declare.

## Acknowledgements

This work was supported by the Gordon and Betty Moore Foundation and the National Science Foundation CBET-1604216.

## Notes and references

1 K. I. Willig, B. Harke, R. Medda and S. W. Hell, *Nat. Methods*, 2007, **4**, 915.
2 S. W. Hell and J. Wichmann, *Opt. Lett.*, 1994, **19**, 780.
3 V. Westphal, S. O. Rizzoli, M. A. Lauterbach, D. Kamin, R. Jahn and S. W. Hell, *Science*, 2008, **320**, 246.
4 M. J. Rust, M. Bates and X. Zhuang, *Nat. Methods*, 2006, **3**, 793.
5 B. Huang, W. Wang, M. Bates and X. Zhuang, *Science*, 2008, **319**, 810.
6 E. Betzig, G. H. Patterson, R. Sougrat, O. W. Lindwasser, S. Olenych, J. S. Bonifacino, M. W. Davidson, J. Lippincott-Schwartz and H. F. Hess, *Science*, 2006, **313**, 1642.
7 M. G. L. Gustafsson, *J. Microsc.*, 2000, **198**, 82.
8 P. J. Keller, A. D. Schmidt, A. Santella, K. Khairy, Z. Bao, J. Wittbrodt and E. H. K. Stelzer, *Nat. Methods*, 2010, **7**, 637.
9 M. G. L. Gustafsson, *Proc. Natl. Acad. Sci. U. S. A.*, 2005, **102**, 13081.
10 L. Schermelleh, P. M. Carlton, S. Haase, L. Shao, L. Winoto, P. Kner, B. Burke, M. C. Cardoso, D. A. Agard, M. G. L. Gustafsson, H. Leonhardt and J. W. Sedat, *Science*, 2008, **320**, 1332.
11 Y. Blau, D. Shterman, G. Bartal and B. Gjonaj, *Opt. Lett.*, 2016, **41**, 3455.
12 D. Li, L. Shao, B. Chen, X. Zhang, M. Zhang, B. Moses, D. E. Milkie, J. R. Beach, J. A. Hammer III, M. Pasham, T. Kirchhausen, M. A. Baird, M. W. Davidson, P. Xu and E. Betzig, *Science*, 2015, **349**(6251), aab3500.
13 F. Ströhl and C. F. Kaminski, *Optica*, 2016, **3**, 667.
14 F. Wei, D. Lu, H. Shen, J. L. Ponsetto, E. Huang and Z. Liu, *Nano Lett.*, 2014, **14**, 4634.
15 F. Wei and Z. Liu, *Nano Lett.*, 2010, **10**, 2531.
16 A. I. Fernández-Domínguez, Z. Liu and J. B. Pendry, *ACS Photonics*, 2015, **2**, 341.
17 J. L. Ponsetto, F. Wei and Z. Liu, *Nanoscale*, 2014, **6**, 5807.
18 J. L. Ponsetto, A. Bezryadina, F. Wei, K. Onishi, H. Shen, E. Huang, L. Ferrari, Q. Ma, Y. Zou and Z. Liu, *ACS Nano*, 2017, **11**, 5344.
19 M. G. L. Gustafsson, D. A. Agard and J. W. Sedat, *Proc. SPIE*, 2000, **3919**, 141.
20 E. Mudry, K. Belkebir, J. Girard, J. Savatier, E. Le Moal, C. Nicoletti, M. Allain and A. Sentenac, *Nat. Photonics*, 2012, **6**, 312.
21 S. M. Mansfield and G. S. Kino, *Appl. Phys. Lett.*, 1990, **57**, 2615.
22 A. Darafsheh, N. I. Limberopoulos, J. S. Derov, D. E. Walker Jr. and V. N. Astratov, *Appl. Phys. Lett.*, 2014, **104**, 061117.
23 Z. Wang, W. Guo, L. Li, B. Luk'yanchuk, A. Khan, Z. Liu, Z. Chen and M. Hong, *Nat. Commun.*, 2011, **2**, 218.
24 H. Yang, R. Trouillon, G. Huszka and M. A. M. Gijs, *Nano Lett.*, 2016, **16**, 4862.
25 P.-Y. Li, Y. Tsao, Y.-J. Liu, Z.-X. Lou, W.-L. Lee, S.-W. Chu and C.-W. Chang, *Opt. Express*, 2016, **24**, 16479.
26 J. Y. Lee, B. H. Hong, W. Y. Kim, S. K. Min, Y. Kim, M. V. Jouravlev, R. Bose, K. S. Kim, I. C. Hwang, L. J. Kaufman and C. W. Wong, *Nature*, 2009, **460**, 498.
27 Y. E. Geints, A. A. Zemlyanov and E. K. Panina, *Opt. Soc. Am. B*, 2012, **29**, 758.
28 A. Darafsheh, C. Guardiola, D. Nihalani, D. Lee, J. C. Finlay and A. Carabe, *Proc. SPIE*, 2015, **9337**, 933705.
29 L. A. Krivitsky, J. J. Wang, Z. Wang and B. Luk'yanchuk, *Sci. Rep.*, 2013, **3**, 3501.
30 E. McLeod and C. B. Arnold, *Nat. Nanotechnol.*, 2008, **3**, 413.
31 K. C. Neuman and S. M. Block, *Rev. Sci. Instrum.*, 2004, **75**, 2787.
32 A. Ashkin, J. M. Dziedzic, J. E. Bjorkholm and S. Chu, *Opt. Lett.*, 1986, **11**, 288.
33 J. Kasim, Y. Ting, Y. Y. Meng, L. J. Ping, A. See, L. L. Jong and S. Z. Xiang, *Opt. Express*, 2008, **16**, 7976.
34 T. A. Nieminen, V. L. Y. Loke, A. B. Stilgoe, G. Knöner, A. M. Brańczyk, N. R. Heckenberg and H. Rubinsztein-Dunlop, *J. Opt. A: Pure Appl. Opt.*, 2007, **9**, S196.
35 J. E. Molloy and M. J. Padgett, *Contemp. Phys.*, 2002, **43**, 241.
36 W. H. Wright, G. J. Sonek and M. W. Berns, *Appl. Phys. Lett.*, 1993, **63**, 715.
37 K. Dholakia and P. Reece, *Nano Today*, 2006, **1**, 18.
38 M. Duocastella, F. Tantussi, A. Haddadpour, R. P. Zaccaria, A. Jacassi, G. Veronis, A. Diaspro and F. Angelis, *Sci. Rep.*, 2017, **7**, 3474.
39 J. Li, W. Liu, T. Li, I. Rozen, J. Zhao, B. Bahari, B. Kante and J. Wang, *Nano Lett.*, 2016, **16**, 6604.
40 S. P. Gross, *Methods Enzymol.*, 2003, **361**, 162.
41 A. Darafsheh, *Ann. Phys.*, 2016, **528**, 898.

 